

# Oxygen Bridge Inhibits Conformational Transition of 1,4-Linked $\alpha$ -D-Galactose Detected by Single-Molecule Atomic Force Microscopy

Qiaobing Xu, Wenke Zhang, and Xi Zhang\*

Key Lab for Supramolecular Structure and Materials, Department of Chemistry, Jilin University, Changchun, 130023, P. R. China

Received July 17, 2001; Revised Manuscript Received October 31, 2001

**ABSTRACT:** A marked shoulder observed around 300 pN in the force–extension curves of  $\lambda$ -carrageenan is a fingerprint of a chair-to-inverted chair conformational transition of the 1 $\rightarrow$ 4-linked  $\alpha$ -D-galactose ring. This shoulder disappears in the force–extension curve when an oxygen bridge is introduced over such a galactose ring in  $\kappa$ - and  $\iota$ -carrageenan. This is due to the spatial barrier of the oxygen bridge resulting in the inhibition of the conformational transition of galactose ring, as predicted by theory. Here we demonstrate it experimentally by monitoring the fingerprint of this conformational transition in the single molecule by atomic force spectroscopy.

## Introduction

With the development of piconewton instrumentation, a series of elegant single-molecule experiments have been carried out, and much new information on the molecular scale has been obtained by taking advantage of atomic force microscopy–single molecule force spectroscopy,<sup>1–3</sup> such as the chair-to-boat conformational transition of individual glucopyranose ring,<sup>1,4–6</sup> the splitting of the helical structure,<sup>7–10</sup> the unfolding of the immunoglobulin titin domain,<sup>2,11</sup> and the host–guest interaction force,<sup>12</sup> even accurately measuring the rupture force of silicon–carbon and sulfur–gold bonds which cannot be obtained accurately by conventional methods.<sup>13</sup> The method has also been extended to study the nanomechanical properties of synthetic polymers and some natural biomaterials.<sup>14–17</sup>

Force-induced transitions between the chair and boat conformers of the glucopyranose ring structure of single polysaccharide molecule have recently aroused increasing interest.<sup>1,4–6</sup> Pyranose-based sugars have two distinct conformations, chair and boat, separated by an energy barrier of about 5–8 kcal mol<sup>–1</sup>.<sup>18</sup> Under an external force, the chair conformer, the most stable conformation of the glucopyranose ring, can transform into a boat conformer after passing over the energy barrier. A conformational change between the chair and boat form of the glucopyranose ring would present a sudden elongation of the molecule in polymers of  $\alpha$ -D-glucopyranose, such as amylose, due to a prominent enthalpic component of the elasticity of the molecule,<sup>1,4–6</sup> as indicated by a marked shoulder in each force–extension curve. This enthalpic component results from an increase in the distance between glycosidic oxygen atoms caused by a force-induced transition between the chair and boat conformations of the glucopyranose ring.<sup>1,4–6</sup> But the 1 $\rightarrow$ 4-linked  $\beta$ -D-glucopyranose, such as carboxymethylcellulose,<sup>5,7</sup> a structure isomer of amylose, will not generate any torque during this conformational transition under an external force as a result of no shoulder appearing in the force extension curves. In the polysaccharides with galactose which has a 1 $\alpha$ –4 $\alpha$ -linked polysaccharide chain, such as pectin, a chair–boat–inverted chair conformational transition would occur under the external force, and a two-step shoulder

would appear in the force curve.<sup>6</sup> Theory predicts<sup>19</sup> that due to the spatial barrier, the force-induced conformational transition of the pyranose ring will not occur if an oxygen bridge is introduced over this ring, but this has not yet been demonstrated experimentally.

Here, taking advantage of an advanced piconewton instrument–single molecule force spectroscopy and monitoring the fingerprint of the conformational transition of galactose, it was possible to demonstrate that the conformational transition is inhibited by the oxygen bridge over the galactose ring.

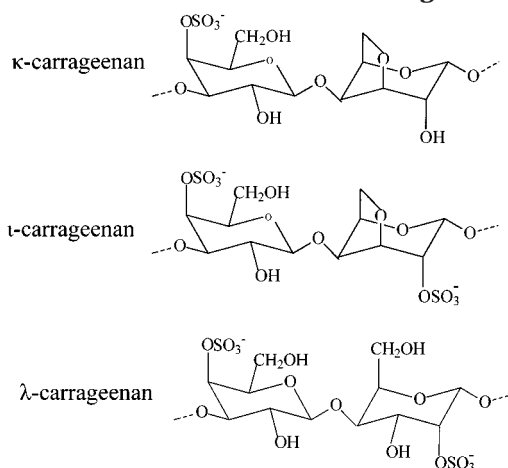
## Experiment Section

**Sample Preparation.**  $\iota$ -Carrageenan from *Eucheuma Spinosa*,  $\kappa$ -carrageenan from *Eucheuma Cottonii*, and  $\lambda$ -carrageenan were all purchased from Sigma. Deionized water was used in all preparation steps and experiments.  $\kappa$ -,  $\lambda$ -, and  $\iota$ -carrageenan were all dissolved in deionized water directly with stirring for half an hour (ambient temperature). The concentration of all samples was about 0.15 mg mL<sup>–1</sup>. About 0.2 mL of solution was cast onto a clean glass slide (1.8 cm  $\times$  1.8 cm), which was cleaned by sonication for about 10 min in toluene, chloroform, acetone, alcohol, and deionized water. The sample was kept in a humid chamber for about 8 h, and then the surplus solution was poured out and rinsed with deionized water. The sample was then used directly for force measurement. Deionized water was used as the buffer in experiment (except special mentioned). The probability to get chain stretching from the sample made above is very small, about 5 in 100 approaching and retracting cycles. This indicates the possibility to obtain the single-molecule stretching upon the sample made above. All experiments were conducted at ambient temperature (about 20  $^{\circ}$ C).

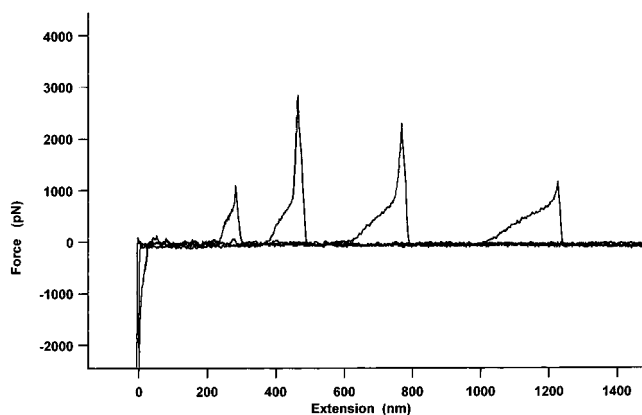
**Force Measurements.** The experimental details on our home-built AFM apparatus have been described elsewhere;<sup>1,2,7,20</sup> it has been demonstrated that the extensibility of individual molecule could be measured. Briefly, when an AFM tip is brought into contact with a polymer sample that was immobilized on a substrate, binding of a single molecule can be achieved due to the molecular dimensions of the tip apex. Upon retraction, the polymer is stretched and the restoring force is measured as a function of the separation distance, resulting in a force–extension curve.

The spring constant of each individual AFM tip (DI, Santa Barbara, CA) was calibrated in solution, by measuring the amplitude of the thermal fluctuations.<sup>21,22</sup> Spring constants varied between 60 and 80 mN/m. The stretching and relaxation rates both are 5.388  $\mu$ m/s in all experiments. Polysaccharide molecules were picked up with an untreated Si<sub>3</sub>N<sub>4</sub> AFM tip.

\* Corresponding author. Fax 0086-431-8923907 or 8980729.

**Scheme 1. Ideally Repeating Units of the Primary Structures of Three Kinds of Carrageenan<sup>a</sup>**

<sup>a</sup> All of them are identical in one part of the repeating unit, the 1,3-linked  $\beta$ -D-pyranose ring. There is an oxygen bridge over the 1 $\rightarrow$ 4-linked  $\alpha$ -D-galactopyranose ring in the other part of the repeating unit of  $\kappa$ - and  $\iota$ -carrageenan, while no such bridge exists in the main chain of  $\lambda$ -carrageenan.

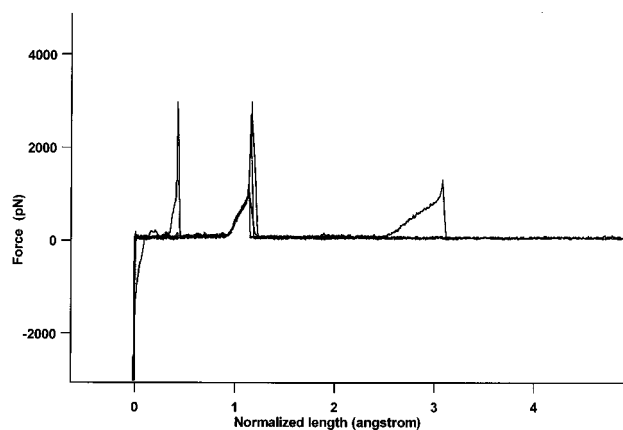
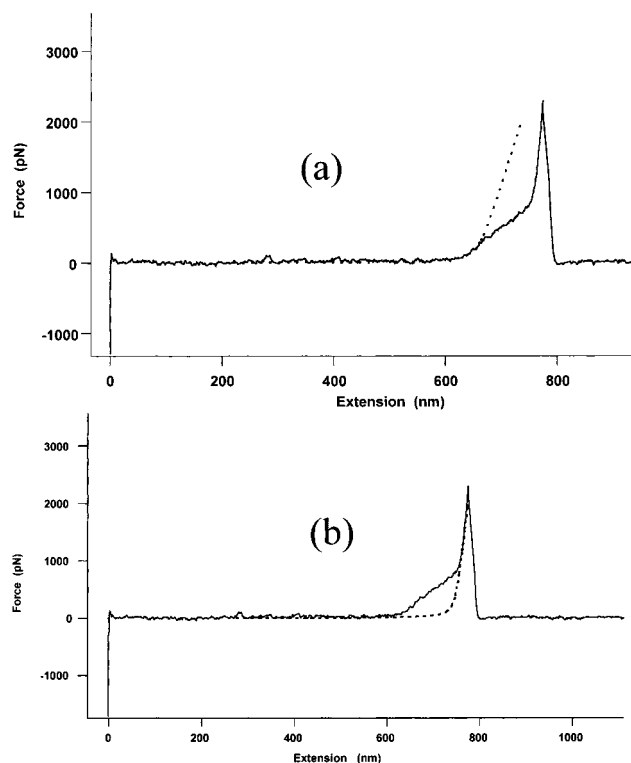
**Figure 1.** Typical force–extension curves with a shoulder of  $\lambda$ -carrageenan.

Since the polysaccharide molecules were not anchored at the ends, the apparent length of the molecule picked up varies.

## Result and Discussion

**Mechanic Properties of  $\lambda$ -Carrageenan.** The primary structure of  $\kappa$ -,  $\iota$ -, and  $\lambda$ -carrageenan are shown in Scheme 1.<sup>23,24</sup> The typical force–extension curve of  $\lambda$ -carrageenan is shown in Figure 1, from which it can be seen that a shoulder about  $300 \pm 50$  pN high appeared in each force–extension curve. Since the polysaccharide sample was polydisperse and the point at which the polymer chain adsorbs to the tip is distributed randomly along the polymer chain, the contour of the polysaccharide chains stretched to different lengths.

To compare the force–extension relationship of polymers of different contour length, the force–extension traces normalized by their lengths and superimposed<sup>1</sup> were plotted in Figure 2. The normalization process was done as usual;<sup>9,10</sup> herein, for each force curve we selected a force value (for example 530 pN), then we obtained a corresponding length value, and after that the extension of the force curve was divided by that length. The good superposition of these curves clearly shows that the elastic properties of such polysaccharide chains scale linearly with the contour length, and all filaments show

**Figure 2.** Well normalization of the force curve shown in Figure 1.**Figure 3.** Force curve with shoulder can be well fitted by the modified FJC model before and after the shoulder (dotted line is the fitted data).

a transition at the same force. This is one of the criteria of single chain stretching.<sup>1,9,16,17</sup>

A modified freely jointed chain (FJC) model was used to describe the extension of the polymer and the entropic restoring force generated.<sup>1,4,16,25,26</sup> The modified FJC model treats a macromolecule as a chain of statistically independent segments of lengths  $l_k$  (Kuhn length), and the segment can be deformed under stress:

$$x(F) = \left[ \coth\left(\frac{Fl_k}{k_B T}\right) - \frac{k_B T}{Fl_k} \right] (L_{\text{contour}} + \frac{nF}{K_{\text{segment}}})$$



where  $F$  is the external force acting on the polymer

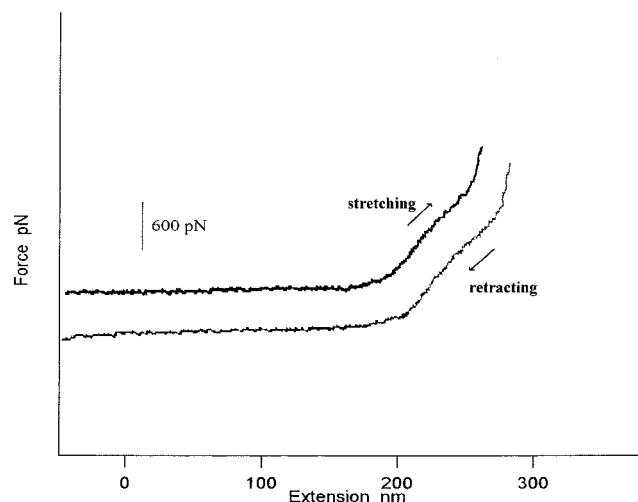


**Figure 4.** Reversible experiment of the single  $\lambda$ -carrageenan elongation, which shows the conformational transition is a reversible process.

chain,  $x$  is the extension of the polymer chain (end-to-end distance),  $L_{\text{contour}}$  is the contour length of the polymer chain,  $n$  is the number of monomers in the filament,  $k_B$  is the Boltzmann constant, and  $T$  is the temperature. The deformability of segments is characterized by a specific parameter, the segment elasticity,  $K_{\text{segment}}$ . The elasticity of a modified FJC chain is dominated by the entropic contribution at low forces, and at high forces the elasticity is dominated by enthalpy.

Although the contour lengths  $L_{\text{contour}}$  of the polymers varied, the force curve obtained from different experiments with different cantilevers all can be fitted by the modified FJC model before the shoulder and after the shoulder. A typical simulation force curve is shown in

Figure 3. The adjustable parameters of the modified FJC model are the Kuhn (segment) length,  $l_k$ , and the elasticity of each individual segment,  $K_{\text{segment}}$ . In the low force region (below the shoulder), the  $\lambda$ -carrageenan molecule is well described by the modified FJC model with a Kuhn length of  $l_k = 1.05$  nm and segment elasticity  $K_{\text{segment}} = 17 \pm 1$  nN nm $^{-1}$ . In the high force region (above the shoulder), it also can be fitted by such model and get  $l_k = 1.18$  nm and  $K_{\text{segment}} = 41 \pm 1$  nN nm $^{-1}$ . On the basis of the good normalization and almost the same fit parameters from the modified FJC fit for all measured  $\lambda$ -carrageenan strands, we believe that predominantly individual filaments are measured in the experiment described.<sup>1</sup>

When single  $\lambda$ -carrageenan molecules were repetitively stretched and relaxed, as shown in Figure 4, there was no hysteresis, indicating that the transition has only a low activation barrier and that the experiment is carried out under equilibrium conditions. To do such reversible experiment successfully, a strand should adsorb onto the tip first and should not detach from the tip before relaxation. The reversible experiment also strongly confirms that such a shoulder is a characteristic property of single  $\lambda$ -carrageenan molecules during the elongation.

Sometimes a force curve such as shown in Figure 5a was obtained. Three force signals appeared. They all show a same character with a shoulder in each signal. This is ascribed to multichain adsorption, the chains being elongated one at a time. Each force signal can be well normalized according to their contour length, as shown in Figure 5b, which further confirms that such a shoulder is a characteristic property of a single  $\lambda$ -carrageenan molecule. We varied the velocity of stretching and relaxing between 0.538 and 5.388  $\mu\text{m/s}$ ; no obvious change is observed in the force curve of  $\lambda$ -carrageenan.

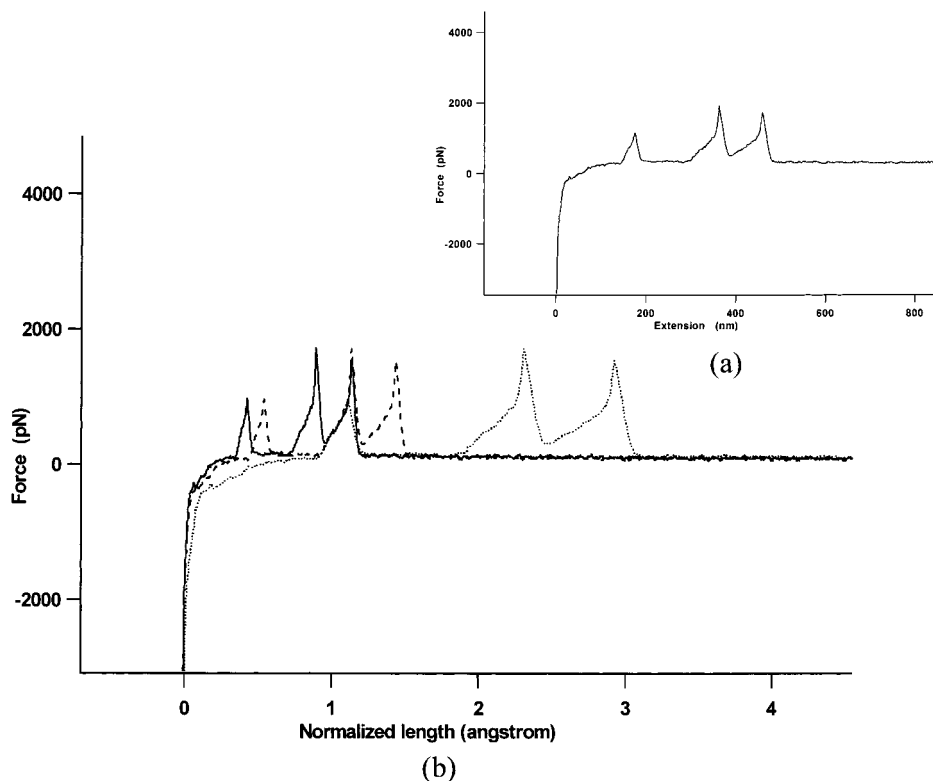


**Figure 5.** (a) Force curve with three force signals shows a shoulder in each force peak. (b) Well normalization of these three force signals.

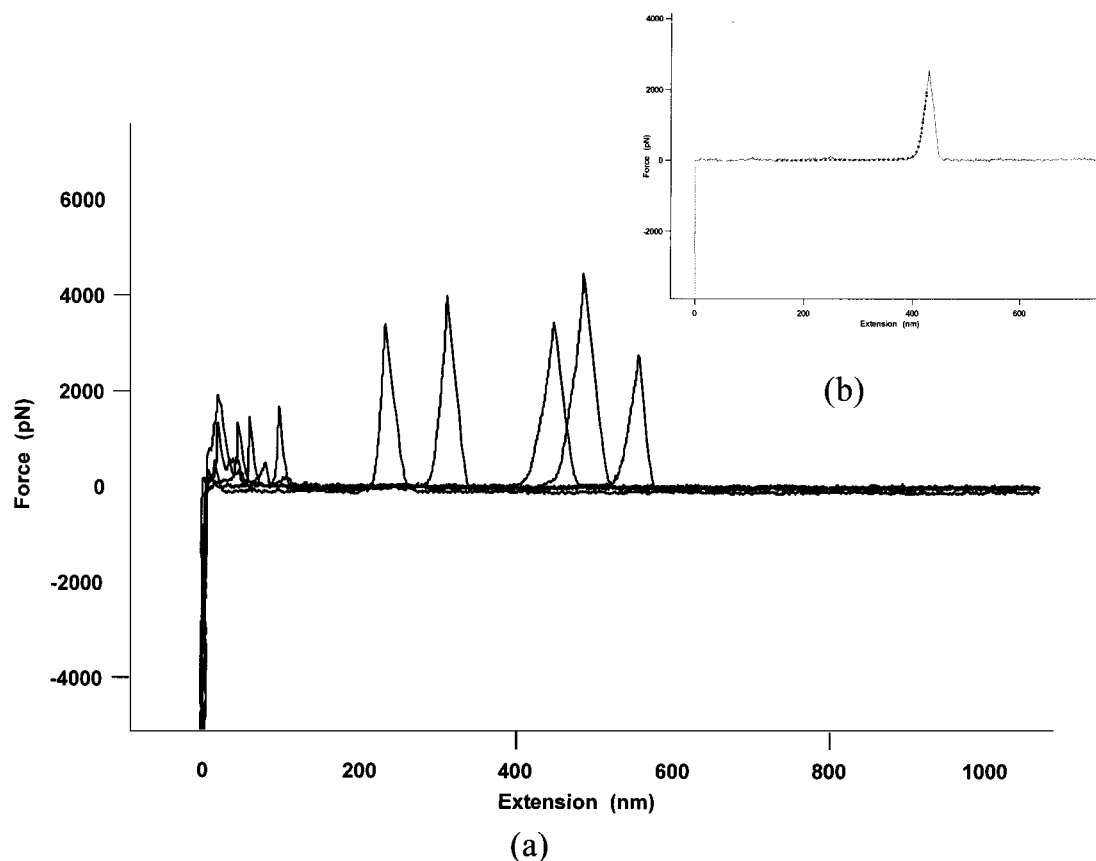


**Figure 6.** (a) Typical force–extension curves of  $\iota$ -carrageenan without a shoulder. (b) Well-fitted force curve of  $\iota$ -carrageenan by the modified FJC model (dotted line is the fitted data).

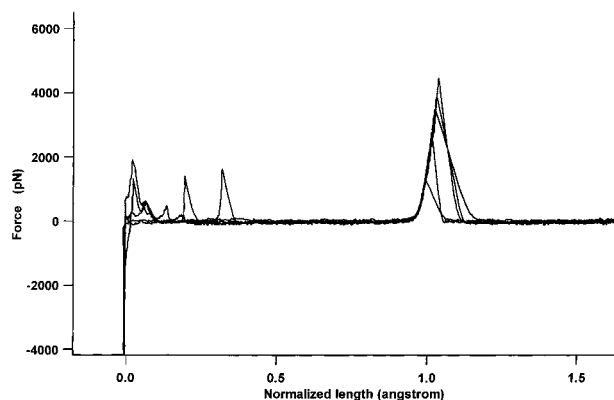


**Figure 7.** Well normalization of the force curves obtained in the  $\iota$ -carrageenan.

**Single-Chain Elongation of  $\iota$ -Carrageenan.** The typical force–extension curve of  $\iota$ -carrageenan is shown in Figure 6a, which shows a sharp increase in each force profile when the extension approaches the contour length of the strand being stretched. The force curve can be well fitted by the modified FJC model as shown in Figure 6b and almost shown the same fitted parameters. The  $K_{\text{segment}}$  of  $\iota$ -carrageenan is around  $40 \pm 2 \text{ nN nm}^{-1}$ , and the Kuhn length is about 1.32 nm. Both the normalization shown in Figure 7 and the use of fitted parameters by the modified FJC reflect the stretching realized of a single chain in the experiment.

**Inhibition of the Conformational Transition of the Galactose by the Oxygen Bridge.** Comparing the force profile obtained of  $\iota$ -carrageenan with those of  $\lambda$ -carrageenan, the remarkable difference is that no marked shoulder appears for the  $\iota$ -carrageenan stretch-

ing. Since the primary structure of these two kinds of carrageenan are the same except for an oxygen bridge in the 1→4-linked  $\alpha$ -D-galactose ring of  $\iota$ -carrageenan, we conclude that the difference of the two kinds of force curves may be ascribed to this oxygen bridge.

Marszalek and Li et al.<sup>1,4–6</sup> have thoroughly studied the force-driven conformational transition of polysaccharides and have shown that the glycosidic bonds are equatorial (e); the torque is zero, causing no conformational change. However, when the glycosidic bond is axial (a), a torque is generated, causing a rotation around C–C bonds and a conformational change.<sup>6</sup> In these three kinds of carrageenan, one part of the repeating units is 1→3-linked  $\beta$ -D-galactose, which has both glycosidic and aglycon bonds in the equatorial orientation. Such a 1e–3e-linked galactose would lead no marked shoulder in the force curve. In  $\lambda$ -carrageenan, the O-4-substituted monomer has both glycosidic and aglycon bonds in the axial orientation, which would lead to a chair–inverted chair conformational transition under the external force and yield a marked shoulder in the force–extension curves, as shown in Figure 1. However, no two-step shoulder has been observed,<sup>6</sup> which may be attributed to the heteropolymer in the main chain of  $\lambda$ -carrageenan.<sup>27</sup> Because of the spatial barrier, this marked shoulder disappears when an oxygen bridge has been introduced over the 1→4-linked  $\alpha$ -D-galactose ring as in  $\iota$ -carrageenan. The force profiles obtained from  $\iota$ -carrageenan are well fitted by the modified FJC (shown in Figure 6b), showing no measurable enthalpic component. Since the force curves of  $\iota$ -carrageenan do not show any marked shoulder which is a criterion of the conformational transition of the 1→4-linked  $\alpha$ -D-galactose ring during the stretching, it

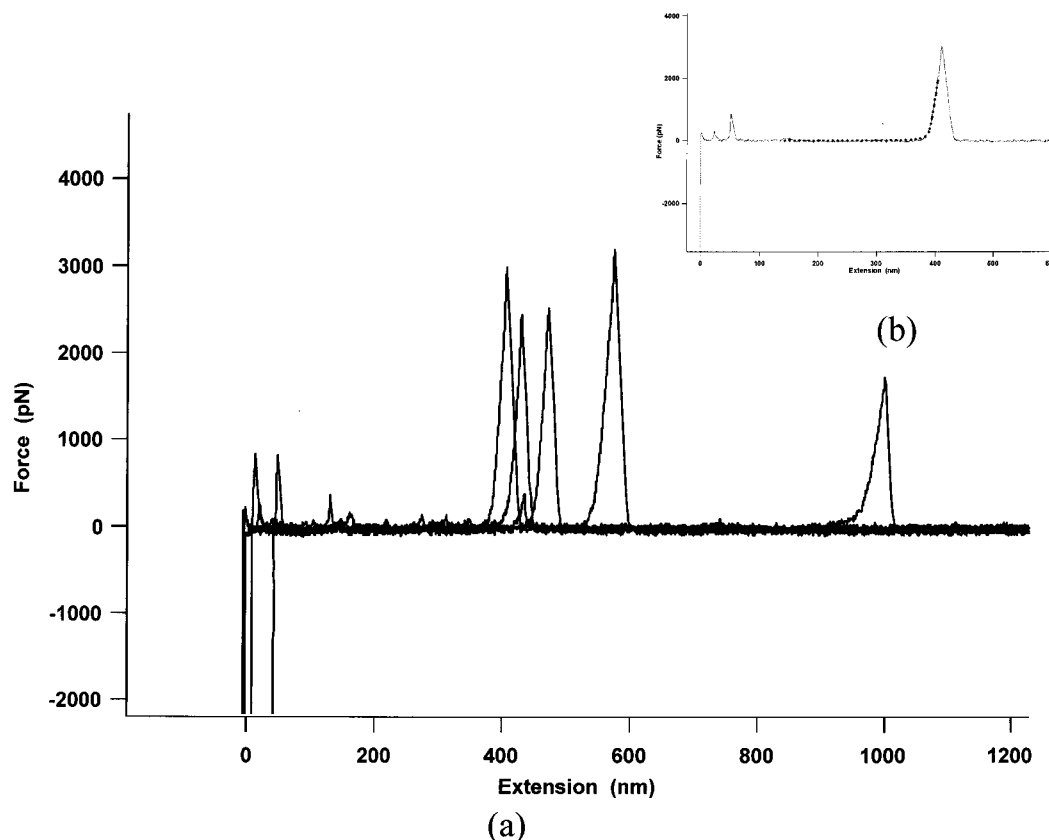


**Figure 8.** (a) Typical force curves obtained from  $\kappa$ -carrageenan similar to those obtained  $\iota$ -carrageenan in shape. (b) Well-fitted force curve by the modified FJC model (dotted line is the fitted data).

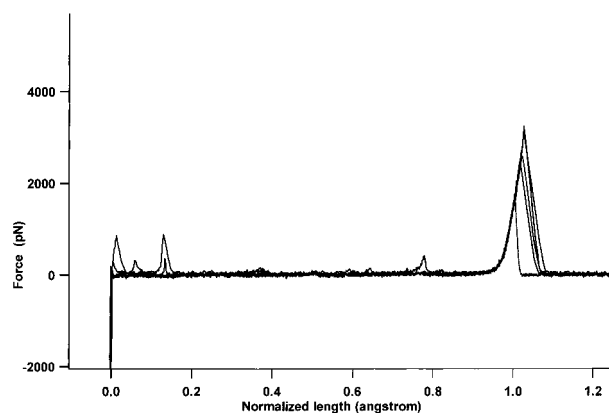


**Figure 9.** Well normalization of the force curve shown in Figure 8a.

may be concluded that the chair-to-inverted chair transition of the 1 $\rightarrow$ 4-linked  $\alpha$ -D-galactose ring in  $\lambda$ -carrageenan is inhibited by the introduction of an oxygen bridge over the galactose ring in  $\iota$ -carrageenan. The stretching and relaxing experiments here also demonstrate that this conformational transition is reversible.

To confirm this hypothesis, we used  $\kappa$ -carrageenan as a control since it contains the same galactose links in the main chain as  $\iota$ -carrageenan, differing only in the number of the sulfate substituent. The force-extension curve in Figure 8a is typical for  $\kappa$ -carrageenan, which shows a similar elastic property, without a measurable enthalpic component, as  $\iota$ -carrageenan. These force curves with different contour length in Figure 8a also can be well normalized as shown in Figure 9. The force curves can also be well fitted by the modified FJC model with same fitting parameters, as illustrated in Figure

8b, indicating that  $\kappa$ -carrageenan behaves like an ideal random coil.<sup>16,17</sup> The segment elasticity of  $\kappa$ -carrageenan is around  $41 \pm 1$  nN nm<sup>-1</sup>, similar to that of  $\iota$ -carrageenan. It is understandable that the mechanical properties of these two polysaccharides are similar since they contain the same galactose rings in the main chain. The absence of a shoulder in the typical force profile of  $\kappa$ -carrageenan further confirms the hypothesis that the disappearance of the marked shoulder in the  $\iota$ -carrageenan is due to the oxygen bridge over the galactose.

In the single-molecule force spectroscopy of PEG and PVA, the force curve with a kink has been observed which is attributed to the unwinding of the inter- or intrachain hydrogen bonds. To eliminate the probability that the shoulder here in  $\lambda$ -carrageenan is also ascribed to the hydrogen bonds, 8 M urea was used in the experiment due to break the hydrogen bonds. However, a similar force curve with a plateau obtained also with the sample in 8 M urea may indicate that the shoulder in the force curve is due to the nature of the main chain, also characterizing conformational transitions in other polysaccharides.<sup>1,4-6</sup>

## Conclusion

By comparing the force-extension curves obtained from the three kinds of native carrageenan, we show that the chair-to-inverted chair transition of the 1 $\rightarrow$ 4-linked  $\alpha$ -D-galactose ring is inhibited by the introduction of an oxygen bridge over the galactose ring. Theoretically, it is understood that this conformational transition of the six-member galactose will be inhibited by the spatial barrier of the oxygen bridge over the galactose ring. Here, we have proven it experimentally by taking advantage of the advanced development of a piconewton



instrument. By studying marked differences in the mechanical properties of the same species and modifying its structure, we may gain an understanding of the nanomechanics and even related functions of biomacromolecules.

**Acknowledgment.** This research was supported by the Major State Basic Research Development Program (Grant G2000078102), Ministry of Education, and Natural Science Foundation of China. We also thank Prof. H. E. Gaub for his kind help in establishing the SMFS setup.

## References and Notes

- (1) Rief, M.; Oesterhelt, F.; Heymann, B.; Gaub, H. E. *Science* **1997**, *275*, 1295–1297.
- (2) Rief, M.; Gautel, M.; Oesterhelt, F.; Fernandez, J. M.; Gaub, H. E. *Science* **1997**, *276*, 1109.
- (3) Janshoff, A.; Neitzert, M.; Oberdörfer, Y.; Fuchs, H. *Angew. Chem., Int. Ed.* **2000**, *39*, 3212–3237.
- (4) Marszalek, P. E.; Oberhauser, A. F.; Pang, Y. P.; Fernandez, J. M. *Nature (London)* **1998**, *396*, 661–664.
- (5) Li, H. B.; Rief, M.; Oesterhelt, F.; Gaub, H. E.; Zhang, X.; Shen, J. C. *Chem. Phys. Lett.* **1999**, *305*, 197–201.
- (6) Marszalek, P. E.; Pang, Y. P.; Li, H. B.; Yazal, J. E.; Oberhauser, A. F.; Fernandez, J. M. *Proc. Natl. Acad. Sci. U.S.A.* **1999**, *96*, 7894–7898.
- (7) Li, H. B.; Rief, M.; Oesterhelt, F.; Gaub, H. E. *Adv. Mater.* **1998**, *10*, 316.
- (8) Rief, M.; Clausen-Schaumann, H.; Gaub, H. E. *Nat. Struct. Biol.* **1999**, *6*, 346.
- (9) Li, H. B.; Zhang, W. K.; Xu, W. Q.; Zhang, X. *Macromolecules* **2000**, *33*, 465.
- (10) Xu, Q.; Zou, S.; Zhang, W.; Zhang, X. *Macromol. Rapid Commun.* **2001**, *22*, 1163.
- (11) Marszalek, P. E.; Lu, H.; Li, H. B.; Carrion-Vazquez, M.; Oberhauser, A. F.; Schulten, K.; Fernandez, J. M. *Nature* **1999**, *402*, 100.
- (12) Schönherr, H.; Beulen, M. J.; Bügler, J.; Huskerns, J.; Van Veggel, F. C. J. M.; Reinhoudt, D. N.; Vancso, F. J. *J. Am. Chem. Soc.* **2000**, *122*, 4963.
- (13) Grandbois, M.; Beyer, M.; Rief, M.; Schaumann, H. C.; Gaub, H. E. *Science* **1999**, *283*, 1727.
- (14) Yamamoto, S.; Tsujii, Y.; Fukuda, T. *Macromolecules* **2000**, *33*, 5995.
- (15) Bemis, J. E.; Akhremitchev, B. B.; Walker, G. C. *Langmuir* **1999**, *15*, 2799.
- (16) Li, H. B.; Liu, B. B.; Zhang, X.; Gao, C. X.; Shen, J. C.; Zou, G. T. *Langmuir* **1999**, *15*, 2120.
- (17) Zhang, W. K.; Zou, S.; Wang, C.; Zhang, X. *J. Phys. Chem. B* **2000**, *104*, 10258.
- (18) Dowd, M. K.; French, A. D.; Reilly, P. J. *Carbohydr. Res.* **1994**, *264*, 1–19.
- (19) Eliel, E. L.; Allinger, N. L. *Topics in Stereochemistry*; Interscience: New York, 1974; Vol. 8, pp 1–95.
- (20) Li, H. B. Ph.D. Thesis, Jilin University, 1998.
- (21) Florin, E. L.; Rief, M.; Lehmann, H.; Ludwig, M.; Dornmair, C.; Moy, V. T.; Gaub, H. E. *Biosens. Bioelectron.* **1995**, *10*, 895–901.
- (22) Butt, H. J.; Jaschke, M. *Nanotechnology* **1995**, *6*, 1.
- (23) Painter, T. J. In *The Polysaccharides*; Aspinall, G. O., Ed.; Academic Press: New York, 1983; Vol. 2, Chapter 4.
- (24) Slootmaekers, D.; De Jonghe, C.; Reynaers, H.; Varkevisser, F. A. *J. Int. J. Biol. Macromol.* **1988**, *10*, 160.
- (25) Smith, S. B.; Cui, Y.; Bustamante, C. *Science* **1996**, *271*, 795–799.
- (26) Smith, S. B.; Finzi, L.; Bustamante, C. *Science* **1992**, *258*, 1122–1126.
- (27) Marszalek, P. E.; Li, H.; Fernandez, J. M. *Nature Biotechnol.* **2001**, *19*, 258–262.

MA011259K